Excitation functions for alpha-particle–induced reactions with natural antimony

N. L. SINGH, D. J. SHAH, S. MUKHERJEE (*) and S. N. CHINTALAPUDI (**)
Physics Department, Faculty of Science
M. S. University of Baroda - Vadodara 390002, India

(ricevuto il 6 Giugno 1996; revisionato il 16 Aprile 1997; approvato il 18 Giugno 1997)

Summary. — Stacked-foil activation technique and γ-rays spectroscopy were used for the determination of the excitation functions of the ^{121}Sb[(α, n); $(\alpha, 2n)$; $(\alpha, 4n)$; $(\alpha, p3n)$; $(\alpha, \alpha n)$] and ^{123}Sb[$(\alpha, 3n)$; $(\alpha, 4n)$; $(\alpha, \alpha 3n)$] reactions. The excitation functions for the production of ^{124}I, ^{123}I, ^{121}I, ^{121}Te and ^{120}Sb were reported up to 50 MeV. The reactions ^{121}Sb$(\alpha, \alpha n) + {}^{123}Sb(\alpha, \alpha 3n)$ are measured for the first time. Since natural antimony used as the target has two odd mass stable isotopes of abundances 57.3% (^{121}Sb) and 42.7% (^{123}Sb), their activation in some cases gives the same product nucleus through different reaction channels but with very different Q-values. In such cases, the individual reaction cross-sections are separated with the help of theoretical cross-sections. The experimental cross-sections were compared with the predictions based on hybrid model of Blann. The high-energy part of the excitation functions are dominated by the pre-equilibrium reaction mechanism and the initial exciton number $n_0 = 4(4p0h)$ gives fairly good agreement with presently measured results.

PACS 25.55 – ^{3}H-, ^{3}He-, and ^{4}He-induced reactions.

1. – Introduction

In alpha-induced reactions the compound nucleus is not formed in a single-step reaction but is reached by a fast nuclear cascade where following the first projectile-target interaction, the few initially excited particles and holes (together called excitons) loose energy by exciting further particles and holes. Generally, particles emitted during this phase of nuclear relaxation have higher energies than those from the subsequent compound nucleus decay, and the chances for pre-

(*) School of Studies in Physics, Vikram University, Ujjain 456010, India
(**) IUC-DAEF Calcutta Centre, 3/LB-8 Bidhan Nagar, Calcutta 700091, India.

equilibrium emission will increase with bombarding energy. Since the pioneering work of Griffin [1], a large number of reaction models have been developed to treat the pre-equilibrium phase of reactions leading to the formation of the compound nucleus from the nuclear system excited at medium energies.

Most of these semi-classical models utilise one way or another the two basic concepts developed in the intranuclear cascade model (INC) [2] and the statistical model of intermediate structure (SMIS) [1]. As a result, a number of formulations, the hybrid model, geometry-dependent hybrid (GDH) model [3-5], the exciton model [6, 7] and many other models [8, 9] have emerged as descendents of Griffin's statistical model of intermediate structure. In later years, there have been far-reaching improvements in the semi-classical or phenomenological models such as hybrid, exciton and index models [10, 11]. These are often used for making comparison with experimental results on account of their simplicity and transparency. Efforts are also in progress to give a fully quantum-mechanical picture of the pre-equilibrium reactions in the framework of multistep theories [12-15] but, due to the complexity of the computation of the interaction of complex particles like an α-particle, the quantum-mechanical picture is yet to come.

Indeed rather extensive experimental data are available in the literature [16-19] for alpha-induced reactions on the antimony using Ge(Li) detector. In view of the mutual discrepancies in the cross-section values for the same reactions, a reinvestigation of the above reactions was undertaken to improve the accuracy on the one hand and to test the various models with systematic experimental data.

2. – Experimental procedure

The excitation functions for antimony were measured using the stacked-foil activation technique and gamma-rays spectroscopy method up to 50 MeV. Natural antimony of spectroscopic purity greater than 99.99% was used for making the targets. Targets are prepared by vacuum evaporation technique of thickness 1.6 mg/cm^2 at the target division of Variable Energy Cyclotron Centre (VECC) Calcutta, India. The stack was formed by placing alternatively 13.5 mg/cm^2 aluminium foils which act as energy degraders. After accounting for the energy degradation in Al foils, the energy of the alpha beam at half the thickness of the experimental foil was calculated from the range energy tables of Williamson *et al.* [20]. The irradiation was carried out at the Variable Energy Cyclotron Centre, Calcutta, India. The beam spot on the foil stack was restricted to 5.0 mm by a central hole in a 6.0 mm thick tantalum collimator placed in front of the stack. The alpha beam was totally stopped in the electrically insulated irradiation head, serving as a kind of Faraday cup, where secondary electrons were prevented from escaping [21]. A beam current of the order of 100 nA was maintained for about 0.5 h. The total alpha-particle beam was collected and measured using a calibrated Ortec current integrator. Using this charge, the flux was calculated.

After irradiation of the stack, the activities produced in the individual foils were recorded using a 120 cm^3 HPGe detector (FWHM 2.0 keV for 1332 keV photons of ^{60}Co), coupled with a 4*k* multichannel analyser. The product nuclei were identified and their yields measured using their characteristic gamma-rays as listed in table I [22]. The energy calibration and efficiency of the detector were determined with a ^{152}Eu standard source obtained from the Radio-Chemistry Division at VECC, Calcutta.

TABLE I. – *Nuclear data used for the identification of residual nuclei.*

Reaction	*Q*-value (MeV)	Half life $T_{1/2}$	Gamma-ray energy E_γ(keV)	% Abundance (θ_γ)
$^{121}_{51}\mathrm{Sb}(\alpha, \mathrm{n})^{124}_{53}\mathrm{I}$	− 07.87	4.15 d	603 723 1691	61.00 10.06 10.49
$^{121}_{51}\mathrm{Sb}(\alpha, 2\mathrm{n})^{123}_{53}\mathrm{I}$	− 15.33	13.02 h	159	82.90
$^{121}_{51}\mathrm{Sb}(\alpha, 4\mathrm{n})^{121}_{53}\mathrm{I}$	− 33.32	2.12 h	212	84.00
$^{121}_{51}\mathrm{Sb}(\alpha, \mathrm{p3n})^{121}_{52}\mathrm{Te}$	− 30.18	16.78 d	573	80.30
$^{121}_{51}\mathrm{Sb}(\alpha, \alpha\mathrm{n})^{120}_{51}\mathrm{Sb}$	− 9.23	5.76 d	1172 1023	100.00 99.10
$^{123}_{51}\mathrm{Sb}(\alpha, 3\mathrm{n})^{124}_{53}\mathrm{I}$	− 23.64	4.15 d	603 723 1691	61.00 10.06 10.49
$^{123}_{51}\mathrm{Sb}(\alpha, 4\mathrm{n})^{123}_{53}\mathrm{I}$	− 31.10	13.02 h	159	82.90
$^{123}_{51}\mathrm{Sb}(\alpha, \alpha3\mathrm{n})^{120}_{51}\mathrm{Sb}$	− 25.01	5.76 d	1172 1023	100.00 99.10

3. – Cross-section determination

The number of observed decays $A_\gamma(t_c)$ is related to the total number of decays $\tau(t_c)$ during the measuring time t_c by

$$A_\gamma(t_c) = P_\gamma(E_\gamma)\, \theta_\gamma(E_\gamma)\, \tau(t_c), \tag{1}$$

where $P_\gamma(E_\gamma)$ is the detector efficiency and $\theta_\gamma(E_\gamma)$ is the absolute γ-ray abundance per decay.

The corresponding reaction yield N_0 is given for simple decays (*i.e.* corresponding to direct production of radioisotopes by the nuclear reactions and we have used only such decays in all the measurements) by

$$N_0 = \tau(t_c)[F(\lambda, t_i, t_w, t_c)]^{-1}. \tag{2}$$

The time dependence is expressed by

$$F(\lambda, t_i, t_w, t_c) = [(1 - e^{-\lambda t_i})(e^{-\lambda t_w})(1 - e^{-\lambda t_c})]/\lambda\,, \tag{3}$$

where $\lambda = \ln 2 / T_{1/2}$ is the decay constant, t_i and t_w are the period of irradiation and period between the end of the irradiation and the beginning of the data collection, respectively.

The related cross-section is defined by

$$\sigma = \frac{N_0}{N_T \phi}, \tag{4}$$

where $N_T = W_i P_i N_{av} / A_i$ is the number of atoms/cm^3 of the target, and ϕ is the total number of alpha-particles used for the irradiation, W_i is the weight per unit area of the target foil; P_i is the fractional abundance by weight of the target isotope of interest. N_{av} is Avogadro's number and A_i is the gram atomic weight of the target element. Hence the formula used for the cross-section calculation is given by

$$\sigma = \frac{A_i A_\gamma \lambda}{\phi \theta_\gamma P_\gamma W_i P_i N_{av} (1 - e^{-\lambda t_i})(e^{-\lambda t_w})(1 - e^{-\lambda t_c})}. \tag{5}$$

The measured cross-sections for the reactions ^{121}Sb(α, n) + ^{123}Sb(α, 3n); ^{121}Sb(α, 2n) + ^{123}Sb(α, 4n); ^{121}Sb(α, αn) + ^{123}Sb(α, α3n); ^{121}Sb(α, 4n); ^{121}Sb(α, p3n) have been listed in table II. The total error in the experimental cross-section is contributed by a photopeak (1–4%), detector efficiency (3–4%), uniformity of the foil thickness (1–2%) and beam current (2–3%). The overall error of our measurement is thus less than 7%. However the above-mentioned error does not include the uncertainties of the nuclear data used in the analysis.

TABLE II. – *Cross-section for the α-induced reactions on* $^{121,\,123}_{51}$Sb.

Target nucleus	$^{121}_{51}$Sb + $^{123}_{51}$Sb	$^{121}_{51}$Sb + $^{123}_{51}$Sb	$^{121}_{51}$Sb	$^{121}_{51}$Sb	$^{121}_{51}$Sb + $^{123}_{51}$Sb
Reaction	(α, n) + (α, 3n)	(α, 2n) + (α, 4n)	(α, 4n)	(α, p3n)	(α, αn) + (α, α3n)
Product nucleus	$^{124}_{53}$I	$^{123}_{53}$I	$^{121}_{53}$I	$^{121}_{52}$Te	$^{120}_{51}$Sb
Threshold energy (MeV)	8.13; 24.4	15.83; 32.11	34.42	31.17	9.53; 25.82
E_α (MeV)	(mb)	(mb)	(mb)	(mb)	(mb)
14.2	122.0 ± 6.2				
16.5	280.9 ± 14.3	23.4 ± 1.3			
21.7	112.9 ± 5.7	809.6 ± 46.5			
25.9	160.7 ± 8.2	1207.0 ± 69.3			3.1 ± 0.2
29.9	679.8 ± 34.6	1069.0 ± 61.4			22.1 ± 1.4
33.1	1112.0 ± 56.6	669.5 ± 38.4			39.0 ± 2.4
36.4	1297.0 ± 66.0	385.4 ± 22.1	15.6 ± 0.9		41.3 ± 2.5
39.5	1078.0 ± 54.9	514.2 ± 29.5	148.2 ± 8.5	73.9 ± 4.2	42.7 ± 2.6
42.5	780.1 ± 39.7	879.7 ± 50.5	576.7 ± 33.1	288.3 ± 16.5	49.5 ± 3.0
45.1	520.8 ± 26.5	1212.0 ± 69.6	1102.0 ± 63.2	657.9 ± 37.8	63.6 ± 3.9
47.7	312.4 ± 15.9	1407.0 ± 80.8	1350.0 ± 77.5	981.2 ± 56.3	82.7 ± 5.1

4. – Results and discussion

Consequent on the use of natural antimony target, which has two isotopes of abundances 57.3% (^{121}Sb) and 42.7% (^{123}Sb), the isotopic contributions arise in the production of a given final nucleus through different reaction channels, for example, ^{124}I is formed in ^{121}Sb(α, n) and ^{123}Sb(α, 3n); ^{123}I is formed in ^{121}Sb(α, 2n) and ^{123}Sb(α, 4n); and ^{120}Sb is formed in ^{121}Sb(α, αn) and ^{123}Sb(α, α3n) reactions, respectively.

However, more often than not, it turns out that at a given energy only one of the two reaction channels is predominant and the other is a small contribution. One of the two vanishes, if the energy happens to be less than the threshold energy for that reaction. On this basis, the experimentally measured weighted average cross-sections can be

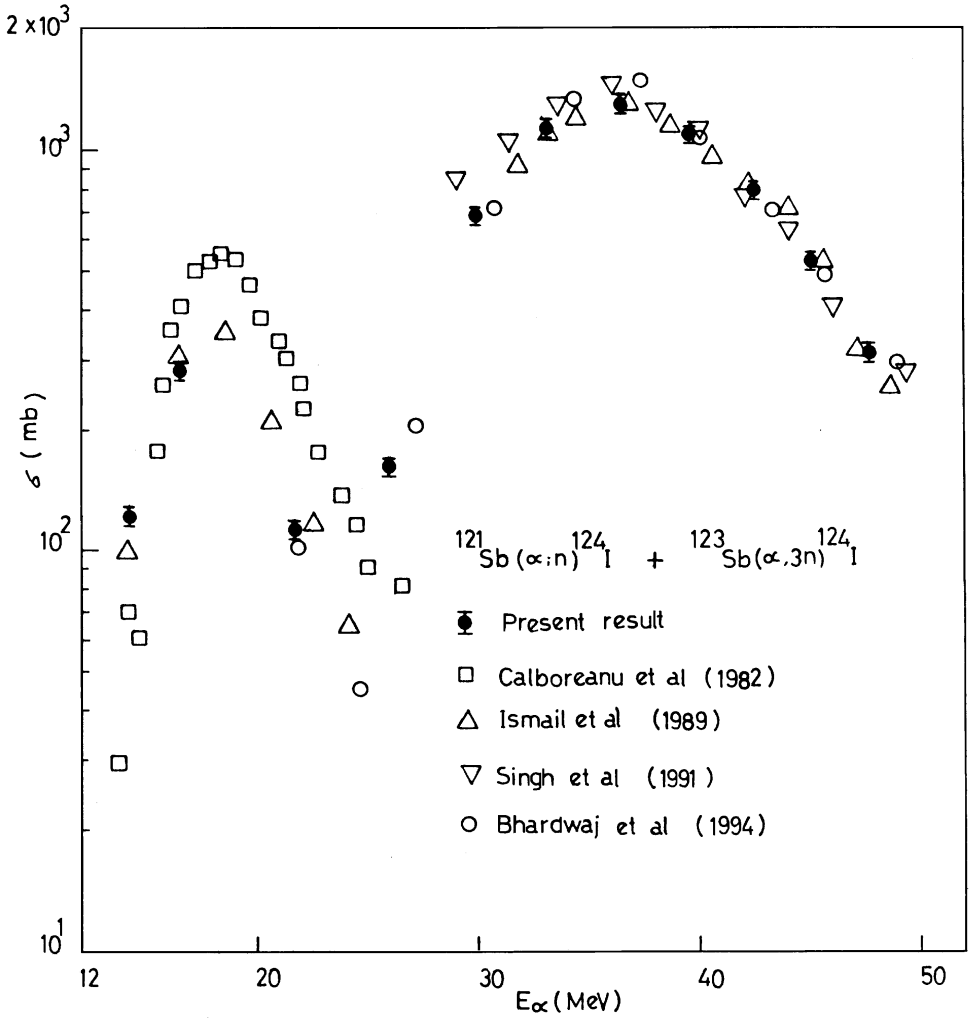

Fig. 1. – Excitation function of the ^{121}Sb(α, n) + ^{123}Sb(α, 3n) reactions.

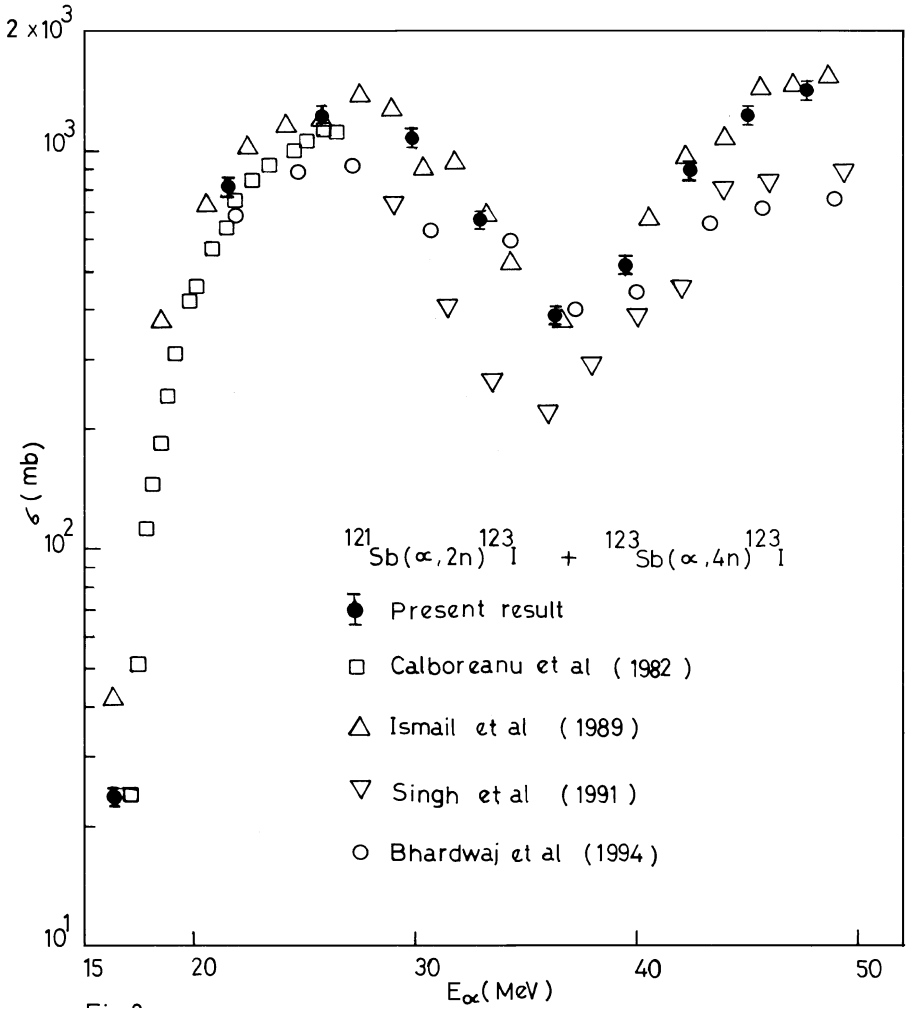

Fig. 2. – Excitation function of the ^{121}Sb(α, 2n) + ^{123}Sb(α, 4n) reactions.

easily interpreted using the formula

$$\langle\sigma\rangle = \overline{A}_i\left(\frac{P_1\sigma_1}{A_1} + \frac{P_2\sigma_2}{A_2}\right), \tag{6}$$

where $\overline{A}_i$ is the average atomic weight of antimony. P_1A_1 and P_2A_2 are the percentage abundance and mass number of two isotopes of antimony in respective order and σ_1 and σ_2 are the individual cross-sections of the reaction ^{121}Sb and ^{123}Sb isotopes, respectively. The two contributions can be separated quite accurately using either the known theoretical ratio of cross-sections [23-25] or by subtracting the contribution of one of the reactions measured with an enriched isotope [26].

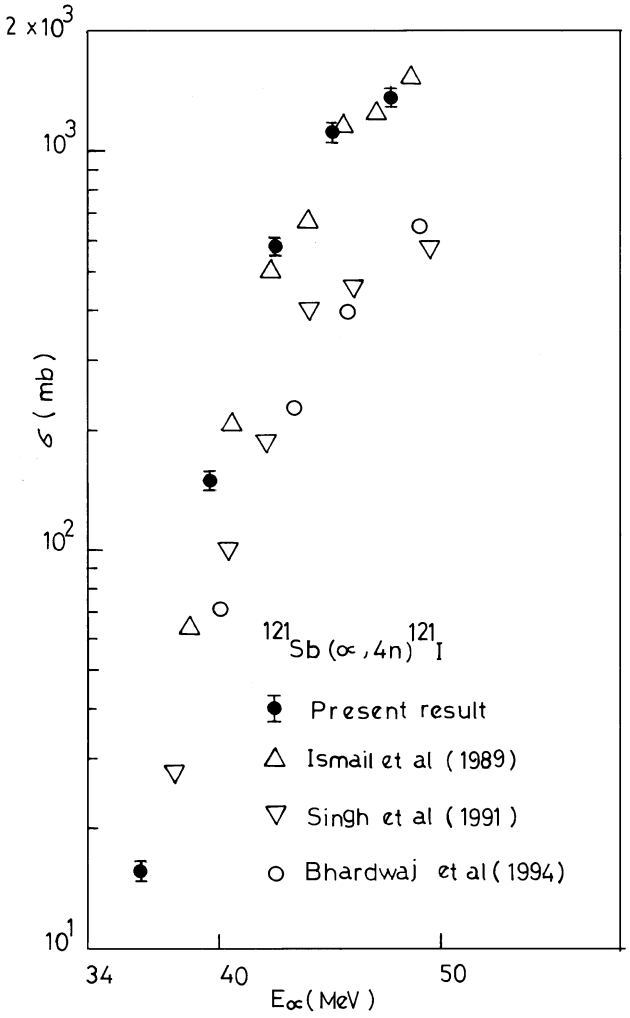

Fig. 3. – Excitation function of the ^{121}Sb(α, 4n) reaction.

Efforts were made to separate the individual contributions of the reactions using the theoretical excitation function in the equations [23]:

$$(7) \qquad \sigma_1 = \sigma^{121}_{(\alpha,\,\mathrm{n})} = \frac{A_\gamma \lambda}{\left[\dfrac{P_i^{121}}{A_i^{121}} + \dfrac{P_i^{123}(\sigma^{123}_{(\alpha,\,3\mathrm{n})}/\sigma^{121}_{(\alpha,\,\mathrm{n})})_{\mathrm{theo}}}{A_i^{123}}\right]} \cdot$$

$$\cdot \phi \theta_\gamma P_\gamma W_i N_{\mathrm{av}} (1 - e^{\lambda t_i})\, e^{-\lambda t_w} (1 - e^{-\lambda t_c})$$

and

$$(8)\qquad \sigma_2 = \sigma^{123}_{(\alpha,\,3n)} = \frac{A_\gamma \lambda}{\left[\dfrac{P_i^{123}}{A_i^{123}} + \dfrac{P_i^{121}(\sigma^{121}_{(\alpha,\,n)}/\sigma^{123}_{(\alpha,\,3n)})_{\mathrm{theo}}}{A_i^{121}}\right]} \cdot$$

$$\cdot \phi\theta_\gamma P_\gamma W_i N_{\mathrm{av}}(1 - e^{\lambda t_i})\, e^{-\lambda t_w}(1 - e^{-\lambda t_c}),$$

where the cross-section ratio $(\sigma^{123}_{(\alpha,\,3n)}/\sigma^{121}_{(\alpha,\,n)})_{\mathrm{theo}}$ and its inverse are taken from the theoretical excitation function calculations based on pre-equilibrium model, which predicts the shape and absolute value of the experimentally measured excitation function.

Below the threshold energy of ^{123}Sb(α, 3n) reaction, the value of $\sigma^{123}_{(\alpha,\,3n)}$ will be zero

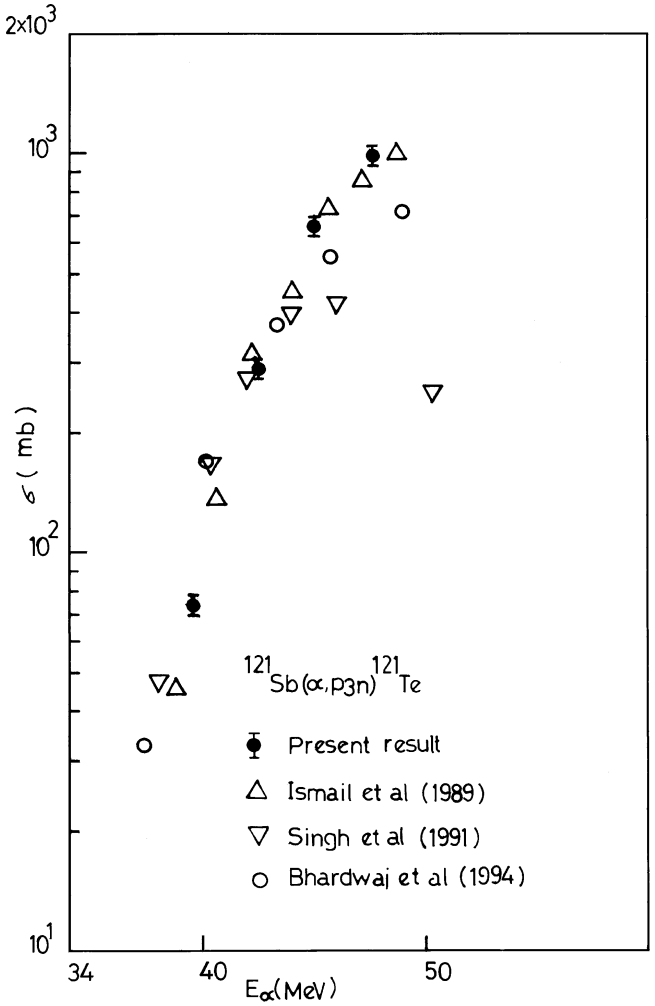

Fig. 4. – Excitation function of the ^{121}Sb(α, p3n) reaction.

and hence the second factor in the square bracket of eq. (7) will be zero. Therefore eq. (7) reduces to eq. (5).

Consequent on the use of natural antimony as the target, two reactions are involved in the production of the residual nucleus ^{124}I. Therefore, the experimental cross-section $\langle\sigma\rangle$ in this case gives the weighted-average cross-section for the two reactions ^{121}Sb(α, n) and ^{123}Sb(α, 3n). Below the threshold energy of ^{123}Sb(α, 3n) (*i.e.* 24.4 MeV) the measured excitation function is due to ^{121}Sb(α, n) reaction only. The contribution of ^{121}Sb(α, n) and ^{123}Sb(α, 3n) reactions beyond 24.4 MeV was separated at each energy using eqs. (7) and (8). Similarly, other reactions which produced the same product nucleus through different reaction channels are separated.

The excitation function for the alpha-induced rections on antimony are shown in fig. 1-4 together with previous results. Calboreanu *et al.* [16] studied the ^{121}Sb(α, n) and ^{121}Sb(α, 2n) reactions up to an alpha-particle energy of 27 MeV. Ismail [17] reported the alpha-induced reactions on antimony up to 58 MeV with an error of 8%. Singh *et al.* [18] measured these reactions up to 60 MeV with an error of 10%. All the previous measurements were carried out with natural antimony employing Ge(Li) detector. From fig. 1-4 it is quite clear that while there is a fair agreement between present measurement and those of Ismail, there is some disagreement between the present results and those of Singh *et al.* and Bhardwaj *et al.*

The cross-sections for the reactions ^{121}Sb(α, αn) + ^{123}Sb(α, α3n) are shown in

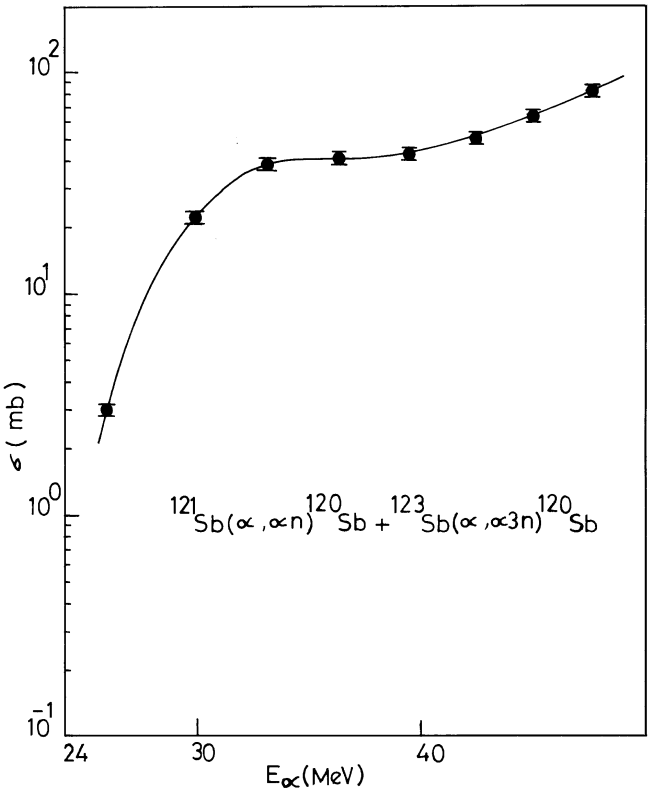

Fig. 5. – Excitation function of the ^{121}Sb(α, αn) + ^{123}Sb(α, α3n) reactions.

fig. 5. To the best of our knowledge, excitation functions for the above reactions are reported for the first time.

The two ^{120}Sb isomers are produced in the ^{121}Sb(α, αn) and ^{123}Sb(α, α3n) reactions with spins (8^-) and (1^+) having half-lives of 5.76 d and 15.8 min and they are genetically independent isomeric states. We have measured the cross-section for the isomeric state having half-life 5.76 d, since the half-life of the other isomeric state is small.

5. – Comparison with theoretical prediction

The excitation functions have been calculated theoretically using the statistical model with and without the inclusion of pre-equilibrium emission of particle using code ALICE/85/300 [27]. The forerunner for this model is the idea of Griffin [1] called the "statistical model of intermediate structure" to qualitatively explain the observed non-Maxwellian structure of continuous particle spectra. This model has been later quantified by deriving the unknown value of the matrix element for binary collision through various means. There are versions called exciton models in which the matrix element is obtained semi-empirically [4] or through a picture of particle-hole interaction in a Fermi sea [6] or by simply treating it as a fit parameter [28]. An attempt to derive it from free nucleon-nucleon scattering cross-sections or from the imaginary part of the optical potential [10] resulted in what are popularly known as the hybrid model versions.

A short description of the option chosen is given below. The nuclear masses were calculated from the Myers and Swiatecki [29] mass formula considering a liquid drop with the shell correction without pairing (*i.e.* the level density pairing is absorbed in the binding energies). The inverse cross-sections were calculated using the optical-model subroutine included in the code which uses the Becchetti and Greenless [30] optical-model parameters. The Fermi level density used is of the form

$$\varrho(u) = (\sqrt{\pi}/12)(u-\delta)^{-5/4} a^{-1/4} \exp\left[2\sqrt{a(u-\delta)}\right],$$

where u is the residual nucleus excitation energy, a is the level density parameter taken as $A/8$ MeV^{-1} which is the default option of the code and $\delta = 11/\sqrt{A}$ MeV the pairing energy shift, with either a back-shifted or standard shift option. We have used the standard option.

There are three main points for discussion when using the hybrid model option of ALICE: i) the initial exciton configuration, ii) the intranuclear transition rate and iii) the mean free path multiplier. In the *a priori* formulation of the hybrid model, the intranuclear transition rates are calculated either from the imaginary part of the optical-model or from the free nucleon-nucleon scattering cross-section [31]. Becchetti and Greenless [30] analysed a vast amount of data to find a best set of optical-model parameters for nucleon-induced reactions. However, for particle energies exceeding 55 MeV, the optical-model parameter of Becchetti and Greenless are no longer applicable and thus at higher energies the mean free path for intranuclear transitions must be calculaed from nucleon-nucleon scattering cross-sections. The mean free path multiplier "k" which is a free parameter originally introduced by Blann [32] to account

for the transparency of nuclear matter in the lower density nucleus periphery was kept equal to unity.

It is customary to use the initial exciton number n_0 separated into proton and neutron excitons (n_p and n_n, respectively) above and a hole n_h below the Fermi level as a fit parameter to match the theoretical predictions with the experimentally observed shape of the spectra and excitation functions. A good guess would be the number of nucleons in the projectile or an additional particle/hole or both [33]. For the incident α-particle used in the present work a reasonable choice for the initial exciton configurations is $n_0 = 4(4\text{p}\,0\text{h})$, $n_0 = 5(5\text{p}\,0\text{h})$ and $n_0 = 6(5\text{p}\,1\text{h})$. All three are tested against the experimentally measured excitation function to pick out the best out of them and to draw inferences based on these comparisons individually for each reaction

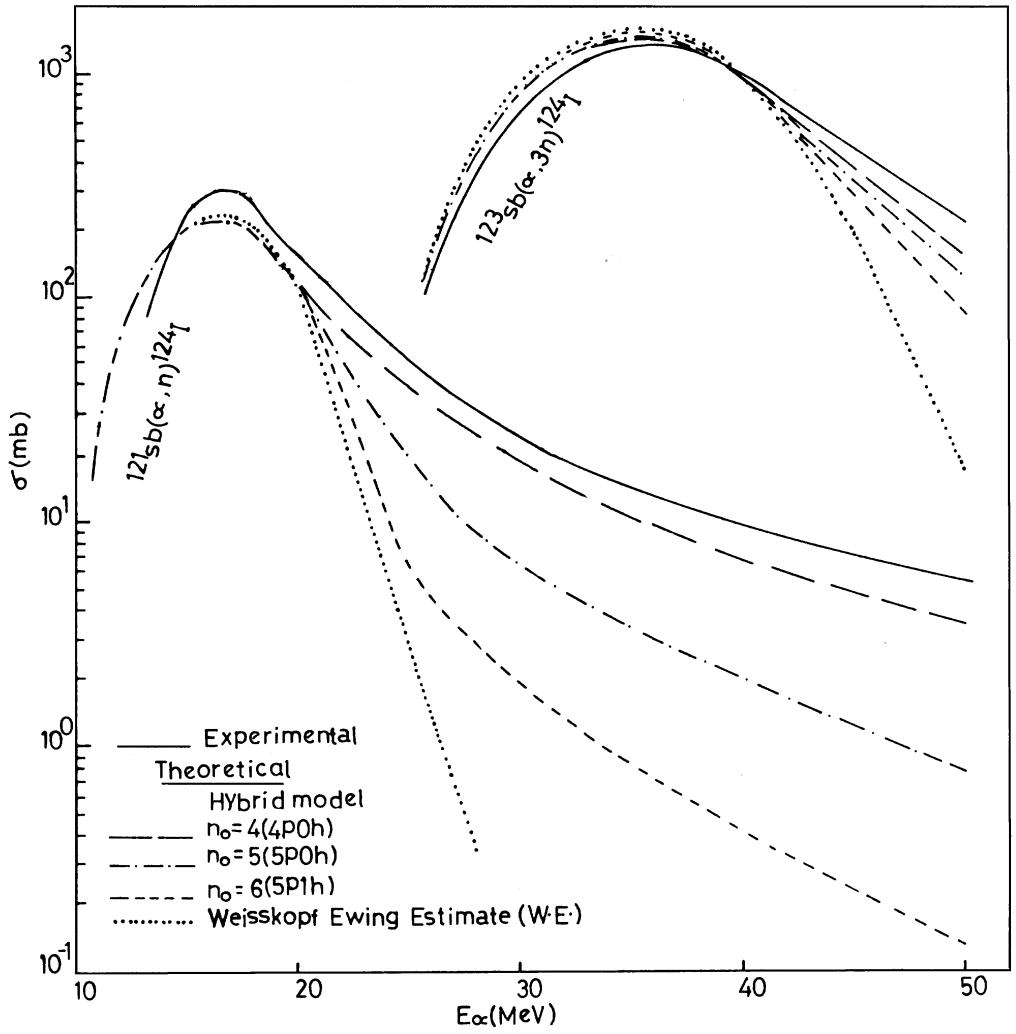

Fig. 6. – Experimental and theoretical excitation function of ^{121}Sb(α, n)^{124}I and ^{123}Sb(α, 3n)^{124}I reactions.

at first. We have made comparisons of experimental results with all initial exciton configurations, where $n_0 = 4(4\mathrm{p}\,0\mathrm{h})$, $n_0 = 5(5\mathrm{p}\,0\mathrm{h})$ and $n_0 = 6(5\mathrm{p}\,1\mathrm{h})$ configurations have been shown by a broken line (— — —), a dot-dashed line (–·–·–), a dashed line (– – –), respectively and Weisskopf-Ewing estimate by dotted line (·····). The lines are drawn only to guide the eye.

Figure 6 shows the experimental and theoretical excitaion functions for the pair of reactions ^{121}Sb(α, n) and ^{123}Sb(α, $3n$) leading to the same residual nucleus ^{124}I. As explained earlier, the individual cross-sections are separated at high energies using eqs. (7) and (8) and shown together with theoretical predictions. Similarly, the excitation functions of the reactions ^{121}Sb(α, 2n) and ^{123}Sb(α, 4n), leading to residual nucleus ^{123}I are separated using eqs. (7) and (8), and shown in fig. 7 together with theoretical predictions. It is observed that Weisskopf-Ewing estimate accounted fairly well for the lower-energy compound-nucleus dominated part of the excitation

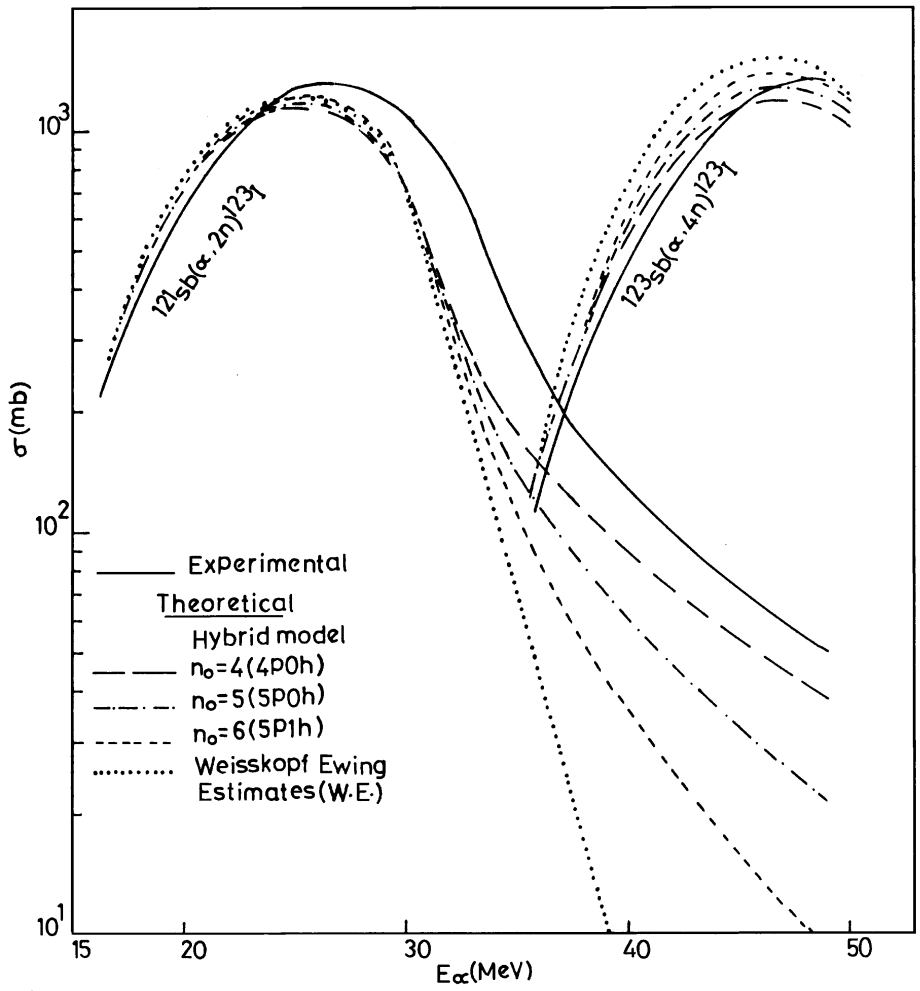

Fig. 7. – Experimental and theoretical excitation function of ^{121}Sb(α, 2n)^{123}I and ^{123}Sb(α, 4n)^{123}I reactions.

functions, but failed to account for the observed cross-sections at high energies where non-equilibrium effects predominate beyond a few tens of MeV of bombarding energy. It can be seen that experimental results are consistent with the theoretical predictions of the hybrid model with an initial exciton number of $n_0 = 4(4\mathrm{p}\,0\mathrm{h})$.

The predictions of the $n_0 = 5(5\mathrm{p}\,0\mathrm{h})$ and $n_0 = 6(5\mathrm{p}\,1\mathrm{h})$ configurations were lower than those obtained with $n_0 = 4(4\mathrm{p}\,0\mathrm{h})$. This is also in agreement with the findings of Djalaeis *et al.* [34], Michel and Brinkmann [35], Gadioli *et al.* [36] who recommended the general application of $n_0 = 4(4\mathrm{p}\,0\mathrm{h})$. The physical interpretation of an initial exciton configuration $n_0 = 4(4\mathrm{p}\,0\mathrm{h})$ is that only four excitons initially share the excitation energy, which is equivalent to a break-up of the incoming alpha-particle in the field of the nucleus and the nucleons occupying excited states above the Fermi energy.

Figure 8 shows the excitation function for $^{121}\mathrm{Sb}(\alpha, 4\mathrm{n})$ and $^{121}\mathrm{Sb}(\alpha, \mathrm{p}3\mathrm{n})$ reactions. The threshold energies for the above reactions are rather large (*i.e.* 34.42 MeV and

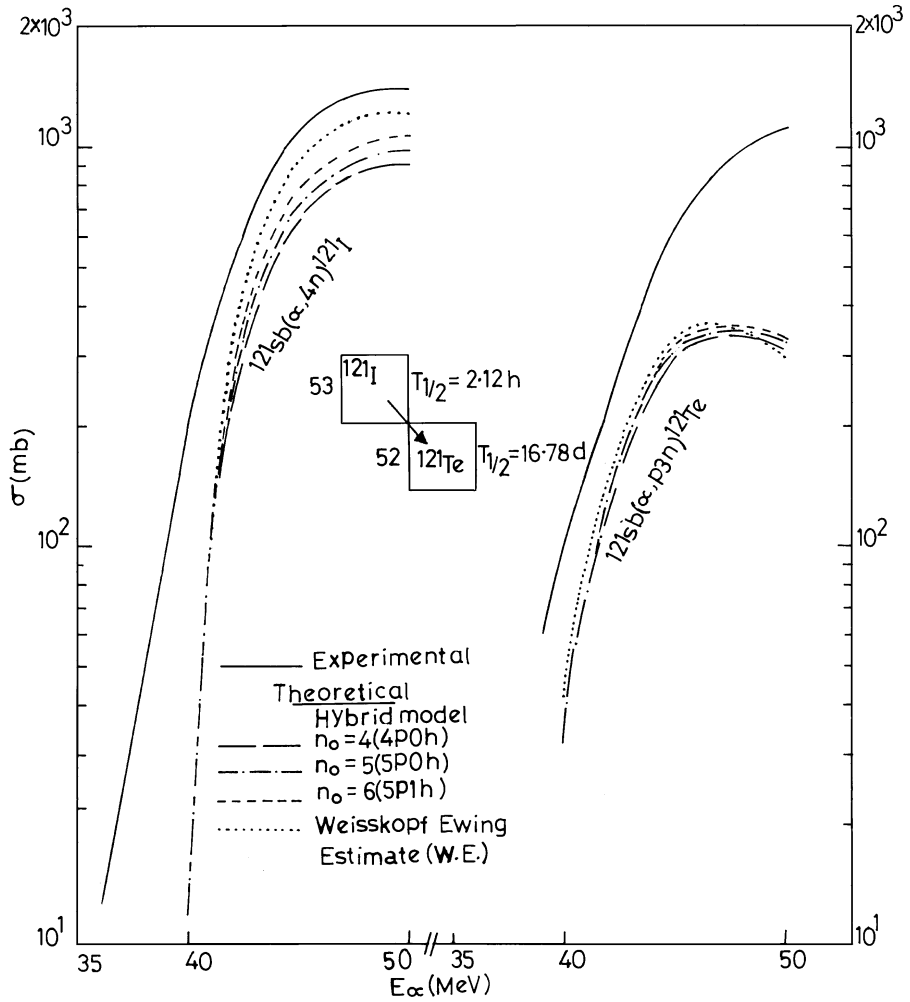

Fig. 8. – Experimental and theoretical excitation function of $^{121}\mathrm{Sb}(\alpha, 4\mathrm{n})^{121}\mathrm{I}$ and $^{121}\mathrm{Sb}(\alpha, \mathrm{p}3\mathrm{n})^{121}\mathrm{Te}$ reactions.

31.17 MeV) and as such there are only a few points in the initial rising part of the experimental excitation functions. In this region the pre-equilibrium model predictions are not very sensitive as the compound-nucleus mechanism dominates. Of all the nuclear particles, neutrons are the easiest to come out of an excited nucleus because they do not feel the Coulomb barrier. Naively, as a rule of thumb, one can say that the cross-sections of the reaction involving neutrons protons and α-particles generally decrease by an order of magnitude down the ladder. For example, the cross-section of ^{121}Sb(α, p3n) reaction is 10 times smaller than that of ^{121}Sb(α, 4n) reaction at comparative energies.

A case in point is the pair of reactions $^{121}_{51}$Sb(α, 4n)$^{121}_{53}$I and $^{121}_{51}$Sb(α, p3n)$^{121}_{52}$Te. Both products being neutron deficient isotopes, naturally the isobar with higher Z decays to that with the lower Z by β^+ emission and/or electron capture. Thus, since both these reactions are energetically possible (their thresholds differ by a couple of MeV) in activation measurements, the cross-sections determined for the lower Z isobar always include the contributions from higher Z isobar. This is evident from the nearly identical values of the cross-sections for the production of ^{121}I and ^{121}Te. The interfering contribution to the (α, p3n) cross-section from that of (α, 4n) reaction is really a major problem specially in view of the fact that the latter cross-section is generally ten times larger than the former.

In the case of ^{121}Sb(α, αn)^{120}Sb + ^{123}Sb(α, α3n)^{120g}Sb, the partial cross-section for the genetically independent isomeric state ^{120m}Sb was not measured in the present work, since the half-life is small nor it is available in the literature. Therefore, no theoretical comparison was attempted for the above reactions.

6. – Fraction of pre-equilibrium particle emission

The present studies clearly show considerable pre-equilibrium contribution in alpha-induced reactions. The pre-equilibrium fraction (f_{PE}) is a measure of the relative weights of the pre-equilibrium and equilibrium components needed to reproduce an experimental excitation function. However, the fractions of pre-equilibrium particle emission for protons and neutrons obtained from the analysis of data are not directly comparable because of the presence of the Coulomb barrier for charged-particle emission. The Coulomb barrier tends to cut off the low-energy portion of proton spectra thus reducing the number of equilibrium protons. There is relatively little effect on the number of pre-equilibrium protons since these tend to be emitted with fairly high energies. The net effect is that as the mass of the compound nucleus increases, the height of the Coulomb barrier increases and the ratio of pre-equilibrium to equilibrium proton emission is increased [4]. It is therefore defined as the integral pre-equilibrium neutron cross-section plus the pre-equilibrium proton cross-section divided by the total compound nucleus cross-section. This quantity is designated by f_{PE}. The calculated f_{PE} for $^{121, 123}$Sb are shown in fig. 9 as a function of bombarding energy (E_α). It is found that f_{PE} increases very fast as the energy of the α-particle increases. Furthermore, the threshold for pre-equilibrium emission is higher for the lower mass number and f_{PE} is higher for the system of higher mass number at a given α-particle energy.

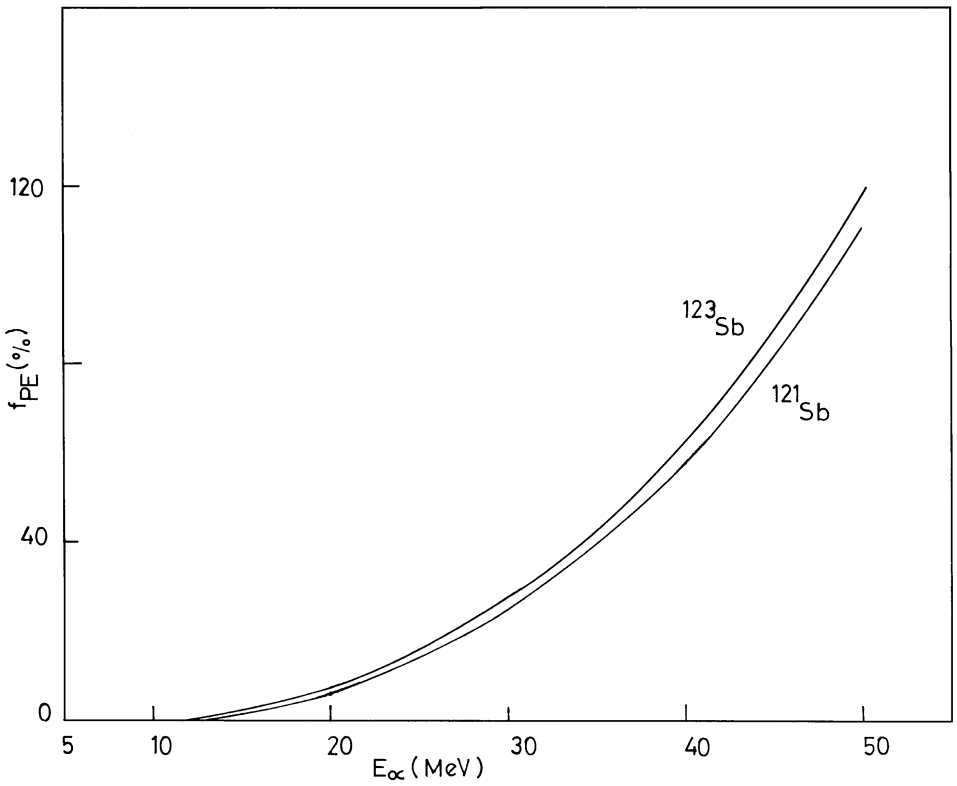

Fig. 9. – Pre-equilibrium fraction (f_{PE}) as a function of incident energy of alpha-particle.

7. – Conclusions

Excitation functions for five reactions of the type (α, xn) and one reaction of the type (α, pxn) and two reactions of the type (α, αxn) were studied up to 50 MeV in the present work. From an overall comparison of the experimental results and theoretical predictions based on compound-nucleus Weisskopf-Ewing estimate as well as hybrid model, one can infer as in other works that the Weisskopf-Ewing estimates accounted well for the low-energy compound-nucleus dominated part of the excitation functions, but failed to account for the observed cross-sections at higher energies.

The emission of nucleons from a nuclear system at excitation energies beyond a few tens of MeV is caused by the pre-equilibrium decay of the system in a time much shorter than the time for evaporation from an equilibrated compound nucleus. This is indirectly indicated by the "high-energy tails" of the experimental excitation functions which signify a less rapid fall for the cross-section than predicted by the compound nucleus model. The shape of the excitation functions in the pre-equilibrium dominated region of energy is fairly well reproduced by an initial exciton configuration $n_0 =$ 4(4p0h). This picture is quite consistent with the basic physics of the pre-equilibrium decay that only a small number of degrees of freedom are initially excited in nuclear reactions at moderate energies.

The pre-equilibrium fraction (f_{PE}) for ^{121}Sb and ^{123}Sb has also been calculated. It is found that the pre-equilibrium reaction increases quickly with the increase of incident alpha-particle energy. The threshold for pre-equilibrium emission is higher for lower mass number. It is also observed that the value of f_{PE} is higher for the system of higher mass number at a given alpha-particle energy.

* * *

We wish to express our sincere thanks to Prof. J. RAMA RAO and Prof. D. R. S. SOMAYAJULU for stimulating discussions and help during the course of this work. We also thank the operating staff of VECC Calcutta and IUC-DAEF Calcutta centre, India, for their cooperation during the course of this work. Thanks are also due to Dr. MD. IQBAL, VECC Calcutta for providing targets. The work was supported by University Grant Commission (UGC), New Delhi, India.

REFERENCES

[1] GRIFFIN J. J., *Phys. Rev. Lett.*, **17** (1966) 478; *Phys. Rev. Lett.*, **24**B (1967) 5.
[2] GOLDBERGER N. L., *Phys. Rev.*, **74** (1948) 1268.
[3] BLANN M., *Phys. Rev. Lett.*, **27** (1971) 337, 700E, 1550E.
[4] CLINE C. K. and BLANN M., *Nucl. Phys. A*, **172** (1971) 225.
[5] BLANN M., *Phys. Rev. Lett.*, **28** (1972) 757.
[6] GADIOLI E., GADIOLI-ERBA E. and SONA P. G., *Nucl. Phys. A*, **217** (1973) 589.
[7] GADIOLI E. and GADIOLI-ERBA E., *Nucl. Instrum. Methods*, **146** (1977) 265.
[8] CLINE C. K., *Nucl. Phys. A*, **210** (1973) 590.
[9] BETAK E. and DOBES J., *Z. Phys. A*, **279** (1976) 319.
[10] BLANN M. and VONACH H. K., *Phys. Rev. C*, **28** (1983) 1475.
[11] ERNST J. FRIEDLAND W. and STOCKHORST H., *Z. Phys. A*, **328** (1987) 333; **333** (1989) 45.
[12] AGASSI D., WEIDENMUELLER H. A. and MANTZOURANIS G., *Phys. Rev.*, **22** (1975) 145.
[13] TAMURA T. and UDAGAWA T., *Phys. Lett. B*, **78** (1978) 189.
[14] FESHBACH H., KERMAN A. and KOONIN S., *Ann. Phys.*, **125** (1980) 429.
[15] FIELD G. M., BONETTI R. and HODGSON P. E., *J. Phys. G*, **12** (1986) 903.
[16] CALBOREANU A., PENCEA C. and SALAGEAN O., *Nucl. Phys. A*, **383** (1982) 251.
[17] ISMAIL M., *Phys. Rev. C*, **41** (1990) 87.
[18] SINGH B. P., BHARDWAJ H. D. and PRASAD R., *Can. J. Phys.*, **69** (1991) 1376.
[19] BHARDWAJ M. K., RIZVI I. A. and CHAUBEY A. K., *Int. J. Mod. Phys. E*, **3** (1994) 239.
[20] WILLIAMSON C. E., BOUJOT J. P. and PICARD J., Centre d'Etudes Nucleaires de Saclay report No. CEA-R 3042 (1966).
[21] SINGH N. L., MUKHERJEE S. and SOMAYAJULU D. R. S., *Nuovo Cimento A*, **107** (1994) 1635.
[22] LEDERER C. M. and SHIRLEY V. S., *Table of Isotopes*, 7th edition (John Wiley and Sons, New York, N.Y.) 1978.
[23] SINGH N. L., AGARWAL S., CHATURVEDI L. and RAMA RAO J., *Nucl. Instrum. Methods B*, **24**/**25** (1987) 480.
[24] RIZVI I. A., BHARDWAJ M. K., ANSARI M. A. and CHAUBEY A. K., *Can. J. Phys.*, **67** (1989) 870.
[25] BHARDWAJ H. D., GAUTAM A. K. and PRASAD R., *Pramana J. Phys.*, **31** (1988) 109.
[26] MISAELIDES P. and MUENZEL H., *J. Inorg. Nucl. Chem.*, **42** (1980) 937.
[27] BLANN M., Code ALICE/85/300, UCID-20169 (1984).

[28] STOCKHORST H., FRIEDLAND W. and ERNST J., *Proceedings of the III International Conference on Nuclear Reaction Mechanism, Varenna, June 14-19, 1982*, edited by E. GADIOLI (University of Milano, Milano) 1982, p. 119.
[29] MYERS W. D. and SWIATECKI W. J., *Nucl. Phys.*, **81** (1966) 1.
[30] BECCHETTI F. D. and GREENLESS F. D., *Phys. Rev.*, **182** (1969) 1190.
[31] BLANN M., *Nucl. Phys. A*, **213** (1973) 570.
[32] BLANN M., *Ann. Rev. Nucl. Sci.*, **25** (1975) 123.
[33] SINGH N. L., MUKHERJEE S., MOHAN RAO A. V., CHATURVEDI L. and SINGH P. P., *J. Phys. G*, **21** (1995) 399.
[34] DJALAESIS A., JOHN P., PROBST H. J. and MAYER-BAERICKE C., *Nucl. Phys. A*, **250** (1975) 149.
[35] MICHEL R. and BRINKMANN G., *Nucl. Phys. A*, **333** (1980) 167.
[36] GADIOLI E., GADIOLI-ERBA E., SAJO-BOHUS L. and TAGLIAFERRI G., *Riv. Nuovo Cimento*, **6** (1976) 1.